

Supersymmetry in the shadow of photini

Masha Baryakhtar,^a Nathaniel Craig,^{b,c} Ken Van Tilburg^a

^a*Department of Physics, Stanford University
Stanford, CA 94306*

^b*Department of Physics, Rutgers University
Piscataway, NJ 08854*

^c*School of Natural Sciences, Institute for Advanced Study
Princeton, NJ 08540*

ABSTRACT: Additional neutral gauge fermions – “photini” – arise in string compactifications as superpartners of $U(1)$ gauge fields. Unlike their vector counterparts, the photini can acquire weak-scale masses from soft SUSY breaking and lead to observable signatures at the LHC through mass mixing with the bino. In this work we investigate the collider consequences of adding photini to the neutralino sector of the MSSM. Relatively large mixing of one or more photini with the bino can lead to prompt decays of the lightest ordinary supersymmetric particle; these extra cascades transfer most of the energy of SUSY decay chains into Standard Model particles, diminishing the power of missing energy as an experimental handle for signal discrimination. We demonstrate that the missing energy in SUSY events with photini is reduced dramatically for supersymmetric spectra with MSSM neutralinos near the weak scale, and study the effects on limits set by the leading hadronic SUSY searches at ATLAS and CMS. We find that in the presence of even one light photino the limits on squark masses from hadronic searches can be reduced by 400 GeV, with comparable (though more modest) reduction of gluino mass limits. We also consider potential discovery channels such as dilepton and multilepton searches, which remain sensitive to SUSY spectra with photini and can provide an unexpected route to the discovery of supersymmetry. Although presented in the context of photini, our results apply in general to theories in which additional light neutral fermions mix with MSSM gauginos.

KEYWORDS: Beyond Standard Model, Supersymmetric Standard Model

Contents

1	Introduction	1
2	Photini	3
2.1	Photini in the UV	3
2.2	Photini in the IR	4
2.3	Photini at the LHC	6
3	Hiding SUSY	8
3.1	Simulation details	8
3.2	Sensitivity of hadronic searches	9
4	Finding SUSY	14
5	Conclusions	17
A	Selection cuts	18

1 Introduction

Thus far no convincing evidence for supersymmetry (SUSY) has been discovered at the LHC. While this by no means excludes supersymmetric extensions of the Standard Model, it begins to challenge the most natural and minimal realizations of supersymmetry as an explanation for the hierarchy between the weak scale and Planck scale. On the other hand, there are compelling hints at both ATLAS and CMS [1, 2] of a new higgs-like state near 125 GeV with approximately Standard Model-like couplings. Should these hints persist and this state prove to be an elementary scalar, supersymmetry remains the most natural explanation for the hierarchy problem consistent with direct and indirect data.

There are a variety of ways in which a supersymmetric explanation of the weak scale may be reconciled with current LHC limits. One possibility is that the entire spectrum of superpartners is moderately tuned, such that sparticles are not yet kinematically accessible at the LHC; perhaps a percent-level (or worse [3, 4]) tuning is palatable to Nature. Another possibility is that the mass hierarchy of scalars is inverted relative to the mass hierarchy of fermions, such that only third-generation scalars are light [5]; in this case direct production limits remain weak but supersymmetric naturalness is robust [6–9].¹

A third possibility – and the focus of this work – is that all superpartners are light but have thus far evaded detection. The most important experimental handle in current supersymmetry searches at the LHC is missing transverse energy (\cancel{E}_T) in the final state; the searches which set the strongest bounds

¹This scenario is still challenged by limits on new contributions to flavor-changing neutral currents (FCNCs), which require a symmetry relating the soft masses of the first two generations; see e.g. [10–13]. A related possibility is for color octet fermions to be relatively heavy, while scalar partners of all three generations are light; this removes one of the primary SUSY production channels and is less constrained by FCNCs, but requires a non-minimal gaugino sector to minimize radiative corrections [14].

on SUSY parameter space use \cancel{E}_T or related variables to distinguish signal from background events [15–18]. Missing energy is a signal of sparticle production if the theory preserves R -parity, in which case the Lightest Supersymmetric Particle (LSP) is absolutely stable and escapes the detector. While in Standard Model processes missing energy arises only from neutrinos and energy mis-measurement, in SUSY processes the lightest stable particle can carry away a large fraction of the energy in the event as \cancel{E}_T , providing powerful discrimination from Standard Model backgrounds. Consequently, the strongest limits on SUSY spectra may be mitigated if the \cancel{E}_T signal is degraded.²

One possibility is to relax the assumption of R -parity. R -parity is motivated by weak-scale dark matter and baryon number conservation, but it may be violated in a manner consistent with proton stability; in this case \cancel{E}_T signatures may be substantially eroded.³ The disadvantage of R -parity violation is that there is typically no convenient candidate for weak-scale dark matter, and some care must be taken to ensure proton stability and minimize flavor violation.

Alternately, R -parity may be a good symmetry of the universe, but sparticle decays still fail to yield substantial \cancel{E}_T due to additional states in the spectrum beyond the fields of the MSSM. If one or more of these new states is lighter than the Lightest Ordinary Supersymmetric Particle (LOSP) of the MSSM, the LOSP is not stable and subsequently decays to the true LSP. In this case there are various avenues for diminishing the missing energy signals. If the mass splittings in these new supermultiplets are small, the phase space for decay products carrying \cancel{E}_T is reduced; this is the mechanism of “stealth supersymmetry” [26, 27]. Stealth SUSY works particularly well for theories with a low scale of supersymmetry breaking, where small splittings are natural and additional multiplets may be motivated by model-building challenges. But another sensible possibility is simply that the fermionic components of the new degrees of freedom are relatively light and mix weakly with MSSM states. In this case, SUSY production at the LHC results in rapid cascade decays to the LOSP, followed by a prompt or displaced decay into the LSP via SM states that carry away a significant fraction of the transverse energy. The diminution of \cancel{E}_T signals in this case is simply a function of supersymmetric naturalness: the LOSP is close in mass to Standard Model states such as W and Z bosons or the higgs.

A cynic might worry that such a scenario would merely be proof that Nature is needlessly obfuscatory, and the existence of new light fermions a crueler version of “who ordered that?” However, we will argue that there is a highly plausible ultraviolet motivation for precisely this scenario in the form of photini, the gauge fermions of Ramond-Ramond $U(1)$ ’s that arise from the dimensional reduction of string theory on topologically complex compactification manifolds [28]. These new states typically have masses around the mass of the bino and interact with MSSM neutralinos through both kinetic and mass matrix mixing. When this mixing is moderate or large the LOSP can decay promptly to lighter photini, with substantial transverse energy carried off by Z bosons or higgses. The potentially high multiplicity of photini makes this mechanism for reducing \cancel{E}_T well-motivated and reasonably effective at weakening current LHC limits. Although our UV motivation comes from photini, the collider phenomenology of additional gauginos mixing with the bino – and their effects on SUSY searches at the LHC – are entirely general. In particular, similar effects may arise due to, e.g., goldstinos [29–31], singlinos [32], or other light $U(1)$ gauge fermions [33].

In this paper we illustrate the consequences of light and moderately mixed photini for collider limits on supersymmetry. We begin in Section 2 by reviewing the ultraviolet motivation and infrared phenomenology of photini, as well as their impact in supersymmetric cascade decays. In Section 3 we

²A complementary idea is to decrease the amount of *visible* energy in an event, which exploits the significant visible energy requirements in frontier SUSY searches; this may occur when, e.g., the spectrum of states is compressed [19, 20].

³For recent discussions germane to the LHC, see [21–25].

consider the effects of photini on reducing limits from SUSY searches with the greatest reach, particularly those involving jets and \cancel{E}_T . Of course, photini do not entirely extinguish SUSY signatures, and their presence in decay chains may introduce additional hadronic or leptonic activity. In Section 4 we consider the most effective searches for the discovery or exclusion of SUSY with photini, of which the same-sign dilepton and $Z+\text{jets}+\cancel{E}_T$ searches are particularly promising.

2 Photini

We begin by reviewing the ultraviolet motivation for photini from string theory constructions, before turning to the infrared effective theory and the effects on conventional SUSY signals at the LHC. Although our study of LHC phenomenology is motivated by the potential multiplicity of photini arising from string compactifications, it bears emphasizing that the consequences for SUSY searches are generic to any scenario in which additional fermions partially mix with the neutral gauginos of the MSSM, such as singlinos, goldstinos, or additional hidden $U(1)$ gauginos.

2.1 Photini in the UV

Realistic string theory constructions typically result in extra-dimensional manifolds with rich and non-trivial topology, including a large number of closed cycles of varying dimensionality. The topological complexity of the compactification manifold in turn leaves its imprint on the spectrum of Kaluza-Klein (KK) zero modes, potentially giving rise to additional light states beyond those of the MSSM. In particular, the higher-rank tensor fields intrinsic to string theory give rise to many zero modes upon compactification, with each zero mode arising from the independent cycles of the internal manifold. While this is an entirely generic phenomenon, in our case the most interesting such tensor fields are the Ramond–Ramond (RR) forms $C_{2,4}$ of type IIB theory of rank 2 and 4, or the RR forms $C_{1,3}$ of type IIA theory of rank 1 and 3, under which only D-branes are charged.

The statistics of the zero modes resulting from compactification depend on the class of the cycle and the rank of the tensor field. For instance, every independent n -cycle gives rise to a scalar KK zero mode in the presence of a rank n form; in certain compactifications this leads to a plethora of light pseudo-scalar fields with axion-like couplings [34, 35]. Similarly, an antisymmetric form of rank n gives rise also to massless vector fields labeled by the independent cycles of dimension $(n - 1)$. As in the scalar case, these vectors are given by integrals of the form over the corresponding cycle. For instance, in type IIB theory each of the 3-cycles Σ_i^3 allow us to define a 4d vector field

$$A_\mu^i = \int_{\Sigma_i^3} C_4 \quad (2.1)$$

by taking three of the four-form indices along the directions of the cycle. These are truly gauge fields, since they inherit a gauge symmetry from the underlying Abelian gauge symmetry of the RR field $C_4 \rightarrow C_4 + d\Lambda_3$.

These abelian gauge multiplets are not inevitably light; they may acquire a high mass from fluxes or be projected away by orientifold planes. However, given the tremendous multiplicity of independent cycles on a realistic compactification manifold, it is not unreasonable to expect a variety of massless $U(1)$ fields to survive to low energies. Indeed, the only objects charged under RR forms are non-perturbative D-brane states, and so the 4d particle states charged under RR $U(1)$ s arise from D-branes wrapping the corresponding cycles; there are typically no light charged states that could higgs the $U(1)$ s.

Without light charged states, at low energies the RR $U(1)$ s interact with the Standard Model fields either through higher-dimensional operators or through renormalizable kinetic mixing with the hypercharge group $U(1)_Y$. Amusingly, the absence of light charged states for RR $U(1)$ s naturally mitigates limits on such kinetic mixing from astrophysics and laboratory searches for millicharged particles [36–39]. Without light charged states, the kinetic mixing between hypercharge and RR photons can be removed by field redefinition without introducing any physical effects, apart from a shift in the hypercharge gauge coupling. However, the situation becomes significantly more interesting in the presence of low energy supersymmetry breaking. In this case massless RR photons are accompanied by their light fermionic superpartners, the so-called photini. Unlike vectors, which are protected by gauge invariance, RR photini acquire masses of order the gravitino mass $m_{3/2}$ as a result of SUSY breaking. If the dominant source of SUSY breaking for the MSSM also comes from gravity mediation, then these photini masses are of the same order as the MSSM soft masses.

As a consequence of a non-trivial photini mass matrix, the mixing of RR photini with the bino cannot be rotated away by the same field redefinition that decouples the vector fields, and thus has observable effects. For the purposes of LHC phenomenology, the significant result of this mixing is the extension of the MSSM neutralino sector by one or more new states mixed with the bino through the gaugino mass matrix. This leads to a variety of possible signatures depending on the amount of mixing and the size of mass splittings between photini, including extended supersymmetric cascades, displaced vertices, and – in the case of a charged LOSP that stops in the detector – out-of-time decays of the LOSP to photini. While these signatures may be spectacular, there is a fairly pedestrian possibility that may be of greater relevance to current LHC limits: light and moderately-mixed photini. In this case, supersymmetric cascades typically end in the LOSP, followed by a prompt and non-displaced decay to one or two of the lightest photini, which then escape the detector. These final decays may substantially erode the \cancel{E}_T present in the event.

2.2 Photini in the IR

Setting aside the UV motivation, we may focus on the IR effective theory of additional $U(1)$ gauge multiplets kinetically mixed with the MSSM. In a supersymmetric theory, kinetic mixing between $U(1)$ s takes the form [40]

$$\mathcal{L}_{\text{gauge}} = \frac{1}{32} \int d^2\theta (W_a W_a + W_b W_b - 2\epsilon W_a W_b,) \quad (2.2)$$

where W_a and W_b are the chiral gauge field strength superfields for the two gauge symmetries (e.g. $W_a = \bar{D}^2 D V_a$ for the $U(1)_a$ vector superfield V_a). We may bring the pure gauge portion of the Lagrangian to canonical form via the shift $W_b \rightarrow W'_b = W_b - \epsilon W_a$. This renders the gauge Lagrangian diagonal,

$$\mathcal{L}_{\text{gauge}} = \frac{1}{32} \int d^2\theta (W_a W_a + W'_b W'_b) , \quad (2.3)$$

and shifts the visible-sector gauge coupling by an amount

$$g_a \rightarrow g_a / \sqrt{1 - \epsilon^2} . \quad (2.4)$$

Note that if there are many photini with large mixings, this may spoil the successful prediction of gauge coupling unification based on measurements at the weak scale.

If there are no light states charged under $U(1)_b$, then this field redefinition has no effect on the interactions of states charged under $U(1)_a$. The hidden sector photon decouples entirely, leaving only

a shift in the hypercharge gauge coupling [41]. However, the story changes when the remainder of the supermultiplet is considered. Although the $U(1)_b$ gauge boson may be decoupled by field redefinitions, the gaugino λ_b may still mix with the visible sector via off-diagonal terms in the gaugino mass matrix [33]. If this mass matrix is not diagonalized by the same field redefinition, the hidden-sector gaugino retains interactions with the visible sector even in the absence of light states charged directly under $U(1)_b$.

Focusing on the gauge fermions, after supersymmetry is broken the mixings between the photini and MSSM gauginos are encoded in the Lagrangian terms

$$\delta\mathcal{L} \supset iZ_{IJ}\lambda_I^\dagger\not{\partial}\lambda_J - m_{IJ}\lambda_I\lambda_J \quad (2.5)$$

where I, J run across the bino \tilde{B} and n photini $\tilde{\gamma}_i$; the Z_{IJ} encode arbitrary kinetic mixing, while the m_{IJ} are soft masses generated by supersymmetry breaking. As with the gauge kinetic terms, the gaugino kinetic terms may be diagonalized via field redefinitions so that $Z_{IJ} \rightarrow \delta_{IJ}$ and $m_{IJ} \rightarrow m'_{IJ}$. If the kinetic terms are made canonical by the transformation $\lambda_I \rightarrow \lambda'_I = P_{IJ}^{-1}\lambda_J$, then we have $m'_{IJ} = P_{IK}^\dagger m_{KL} P_{LJ}$ and mixing persists in the mass matrix. Moreover, since the final physical mixing among the gauginos depends on the mass matrix mixing, the gauge-coupling unification constraint on the amount of kinetic mixing with hypercharge does not limit the size of the mixing among gauginos.

To study the neutralino mass eigenstates, we diagonalize the gaugino mass matrix \mathbf{m} via $\mathbf{m}_D = \mathbf{U}^*\mathbf{m}\mathbf{U}^{-1}$, where \mathbf{U} is a unitary matrix. The mass eigenstate neutralinos \tilde{N}_I may then be written as

$$\tilde{N}_I = U_{IJ}\lambda_J \quad (2.6)$$

where $I, J = 1, \dots, n+4$ runs over the four MSSM neutralinos and the n photini; U_{IJ} are the components of the matrix \mathbf{U} , and $\lambda_I = (\tilde{B}, \tilde{W}, \tilde{H}_d, \tilde{H}_u, \tilde{\gamma}_1, \dots, \tilde{\gamma}_n)$ are the gauge eigenstate gauginos with canonical kinetic terms. As long as the mixing is not $\mathcal{O}(1)$, the neutralinos decompose into mostly-MSSM and mostly-photino states. Consequently, we may think of the \tilde{N}_a ($a = 1, \dots, 4$) as mostly-MSSM neutralinos, and the \tilde{N}_i ($i = 5, \dots, n+4$) as mostly-photino neutralinos. For the most part, we need not concern ourselves with the majority of the photini. If mixing is large, the effects on collider phenomenology are dominated by one or two photini at the bottom of the spectrum; transitions through heavier photini are kinematically suppressed.

In this work we restrict our attention to the case where mixing is relatively large and erosion of \not{E}_T is maximized: $\epsilon_i \gtrsim 0.1$. Although our interest lies in collider physics, there are several noteworthy consequences for phenomenology. Mixing of this order, while large, is consistent with gauge coupling unification, since it only results in a percent-level shift in the hypercharge gauge coupling. As long as there are no more than a few such strongly-mixed photini, this correction to gauge coupling unification is smaller than typical threshold corrections. And as noted above, the dominant contribution to mixing may not even come from kinetic terms, in which case even this constraint is mitigated.

Large mixing also has favorable consequences for cosmology if the strongly-mixed photini are the lightest in the spectrum. Generic photini with small mixings make poor dark matter candidates, since their thermal relic abundance scales as ϵ^{-4} times the equivalent bino abundance, leading to a substantial overdensity of dark matter (though this improves to an ϵ^{-2} scaling if the photino LSP is close enough in mass to the higgsino for efficient coannihilation). For weakly-mixed photini this requires an alternative cosmology or non-thermal origin for the dark matter relic abundance. But if the LSP photino mixing parameter is $\gtrsim 0.1$ the thermal relic abundance may itself be adequate,

particularly if coannihilation is effective.⁴ In this respect, a few light photini with large mixing are favorable for more than just LHC phenomenology.

2.3 Photini at the LHC

The addition of light photini to the supersymmetric spectrum can effectively hide SUSY at the LHC by reducing the \cancel{E}_T of events with supersymmetric particles. In the presence of photini, the lightest particle in the MSSM can decay further to these light states through Z or higgs boson emission. If the photini are light and have large mixing with the bino (i.e. the bino decay is prompt), then the bosons will carry away most of the energy of the bino as SM decay products, dramatically reducing the missing transverse energy in an event and thus the efficiencies of experimental searches. To see this explicitly, consider the two-body decay of a bino into a Z and a light relativistic photino (in the rest frame of the bino). Then the fraction of the bino energy carried away by the photino is

$$\frac{E_{\tilde{N}}}{E_1} = \frac{m_1^2 - m_Z^2}{2m_1^2} + \mathcal{O}\left(\frac{m_{\tilde{N}}^2}{m_Z^2}\right), \quad (2.7)$$

where $m_1 - m_{\tilde{N}} > m_Z \gg m_{\tilde{N}}$ and m_1, m_Z , and $m_{\tilde{N}}$ are the bino, Z and photino masses, respectively. The fraction tends to zero when the bino mass approaches that of the Z boson. To get the total \cancel{E}_T in a typical SUSY event at the LHC, one has to sum up the momenta of the photini and any neutrinos from Z decays on both sides of the SUSY decay chain, and take the transverse component of this four-momentum sum. Hence the missing energy reduction of (2.7) degrades somewhat, but roughly persists when the binos are only moderately boosted and have momenta oriented in uncorrelated directions. If the bino decay occurs dominantly through light higgs (rather than Z) emission, there is no irreducible \cancel{E}_T from the $\sim 20\%$ branching ratio of Z 's to neutrinos, reducing the total \cancel{E}_T even further (though of course there is still a fraction of \cancel{E}_T in higgs decay products as well).

Since most SUSY searches at particle accelerators look for events with a large amount of \cancel{E}_T , this extra step in the decay cascade tends to diminish the SUSY signal in the canonical ATLAS and CMS searches. We show that this effect significantly weakens the exclusion limits on SUSY from the most constraining hadronic searches at ATLAS and CMS in the next section.

For concreteness, we consider a SUSY spectrum with a mostly-bino LOSP (the mass eigenstate \tilde{N}_1). The mixings between photini and the bino, inherited from the kinetic mixings of the massless $U(1)$ fields, lead to a main decay channel through Z -boson emission: $\tilde{N}_1 \rightarrow \tilde{N}_i + f\bar{f}$. If the Z is produced off-shell, the decay rate is of the order

$$\Gamma(\tilde{N}_1 \rightarrow \tilde{N}_i + f\bar{f}) \simeq \frac{1}{192\pi^2} \frac{\alpha_W}{c_W^2} \eta^4 \epsilon_i^2 \frac{(\delta m_i)^5}{m_Z^4} \text{Br}(Z \rightarrow f\bar{f}), \quad (2.8)$$

where $\delta m_i = |m_1 - m_i|$ is the mass splitting between the bino and the i -th neutralino and the parameter $\eta \sim \mathcal{O}(m_Z/M_{1,2}) \sim \mathcal{O}(m_Z/\mu)$ characterizes the size of the mixings of the bino and higgsinos in the MSSM. In the spectra we consider here, $\eta \gtrsim 0.1$. For a generic case where mixing parameters ϵ_i of the photini are of the same order, we can see from (2.8) that the decay to the lightest photino will in general dominate. In the case of gravity mediation, photini masses are of the same order as soft masses in the MSSM, and for topologically complex manifold compactifications which produce a multitude

⁴We note that coannihilation is unavailable in the detailed spectra considered in this paper due to the lightness of the photini, but simply wish to emphasize the favorable cosmology of this parametric limit.

of photini, generically one or more of the lightest neutralino mass states will have a mass below the bino- Z mass splitting, $|m_i| < m_1 - m_Z$.⁵

In this case, the Z -boson is on-shell and the decay rate is given by [42]

$$\Gamma(\tilde{N}_1 \rightarrow \tilde{N}_J + Z) \simeq \frac{\alpha_W}{2c_W^2} \eta^4 \epsilon_i^2 \frac{(m_1 - m_Z)^2}{m_1} \quad (2.9)$$

for $m_i \ll m_1, m_Z$. Another possibility is for the decay to go through the lightest neutral higgs,

$$\Gamma(\tilde{N}_1 \rightarrow \tilde{N}_J + f\bar{f}) \simeq \frac{\alpha_W}{2} \eta^2 \epsilon_i^2 \frac{(m_1 - m_H)^2}{m_1} \quad (2.10)$$

again for $m_i \ll m_1, m_H$. The relative ratio between higgs decays and Z decays depends on the mixing in the neutralino matrix and the relevant mass splittings.⁶

Other subleading decays for the LOSP are through intermediate squarks and sleptons, or loop-suppressed photon emission; these processes produce similar reduction in SUSY limits but have different discovery channels. For the parameters considered in this work, these ancillary processes are unimportant. In particular, although there may be two-body decays of the LOSP via a photon, the couplings of photini to the photon are suppressed by an additional loop factor. Since (for the spectra considered here) decays involving photons compete with open two-body decays to the Z or higgs, they are substantially suppressed and typically do not provide interesting limits from e.g. $n\gamma + \cancel{E}_T$ searches. In this sense the phenomenology of the MSSM with light photini is substantially different from that of gauge mediation, where two-body LOSP decays involving photons often dominate.

If the bino undergoes a cascade decay through several photini, missing energy becomes converted into Z or higgs decay products at every step of the cascade. In Figure 1(a) we present the missing energy distribution for the case that the bino-like \tilde{N}_1 is the true LSP versus the LOSP that can decay through a chain of 1 or 2 photini via Z bosons. We consider a sample simplified spectrum with $m_{\tilde{g}} = 750$ GeV, $m_{\tilde{N}_1} = 150$ GeV and photini at 20 GeV and 5 GeV. The second Z is far off-shell in the 2-photini cascade, so the reduction in missing energy between steps 1 and 2 is relatively smaller. Adding more steps to the cascade will further decrease the missing energy and hide the signal, but for a generic selection of kinetic mixings between photini, the decay to the lightest state or lightest two states will generally dominate. Therefore, we only consider decays to one or two relatively light photini with masses 5 GeV and 20 GeV.

Missing energy can be dissipated in a decay chain of several photini; usually even one photino is sufficient to dramatically reduce the missing energy in an event. In Figure 1(b) we present the missing energy spectrum in the same model, with the \tilde{N}_1 decaying through a Z in one step to a photino of mass 20 GeV or 5 GeV; since the Z is on-shell in both cases and the photini are much lighter than the bino, there is little difference between the two cases. In the remainder of the paper we will consider a single 5 GeV photino model, which generalizes to other masses as is clear from Figure 1(b). In Figure 1(c), we see that higgs emission is even more efficient at reducing \cancel{E}_T than Z emission; this is due to the fact that the Z decays invisibly to neutrinos 20% of the time, while the higgs is heavier thus carrying

⁵In gauge mediation the photini masses may be significantly lighter, of order the gravitino mass. In this case the phenomenology changes qualitatively due to the presence of the gravitino at the end of SUSY decay chains, and is likely to resemble that of goldstini [29–31]. While potentially very interesting, we will not consider the gauge-mediated scenario in detail here.

⁶Here we assume h is the lightest scalar in the higgs sector. Of course, as the mass of the LOSP increases, it is also possible for decays to involve the heavier higgs states A, H , and H^\pm . For simplicity, we take these states to be decoupled, though including them does not radically change the phenomenology.

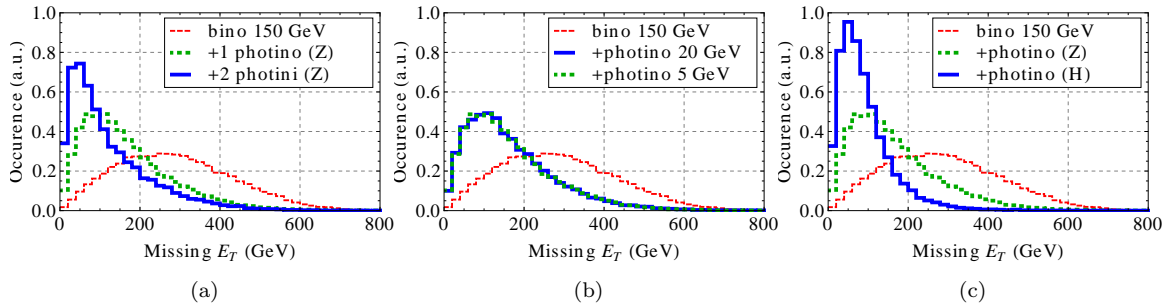


Figure 1. \cancel{E}_T histograms for different photini spectra. We present the effect of (a) number of photini in the decay chain: no photini, one 5 GeV photino or cascade through 20 GeV and 5 GeV photini; (b) mass of the lightest photino; (c) the SM particle in the cascade: bino to Z + photino or bino to 125 GeV higgs + photino. The SUSY model is a simplified spectrum with a 750 GeV gluino and 150 GeV bino LOSP, with the rest of the sparticles decoupled; this benchmark point is currently excluded by experiment as a standard scenario but allowed in the presence of photini.

away a larger fraction of the bino’s energy and has a much smaller fully invisible branching fraction.

3 Hiding SUSY

In this section, we explore the phenomenology of photini in more detail in the context of current ATLAS and CMS hadronic searches. In Section 3.1 we describe the example SUSY spectra we use for our analysis and the implementation of our Monte Carlo-based simulation, while in Section 3.2 we probe the change in exclusion limits of current hadronic searches for SUSY at the LHC in the presence of photini. Although presented in the context of photini, our results may be generalized to any theory in which one or more additional light fermions mix moderately with the bino, such that SUSY cascades proceed through a bino to the LSP via emission of on-shell Z or higgs bosons.

3.1 Simulation details

In order to accurately analyze how photini affect experimental limits on supersymmetry, we consider the leading experimental searches with jets and \cancel{E}_T [15–18] and compare models with a standard neutralino LSP and with photini. The mechanism by which photini alter LHC limits is general for any SUSY model with a neutralino LOSP; in this paper, we focus on three frequently-presented parameter sets which allow direct comparison with existing experimental exclusion limits:

1. a simplified model with a gluino, first- and second-generation squarks and a light bino LOSP, with the remainder of the sparticles decoupled at 3.5 TeV [43, 44].
2. a simplified model with a gluino and bino LOSP with the remainder of the sparticles decoupled at 3.5 TeV [43, 44].
3. the constrained MSSM (cMSSM) model [45–50] with a mostly-bino LOSP, with parameter choices $A_0 = 0$, $\tan \beta = 10$, and $\mu > 0$ for varying values of m_0 and $m_{1/2}$. The low energy spectra are generated with SOFTSUSY 2.0.18 [51].

We use the superspace module of Feynrules v1.4.0 [52] (altered to include the dynamics of extra abelian superfields without light charged matter under them) to incorporate the photini \tilde{N}_i in UFO

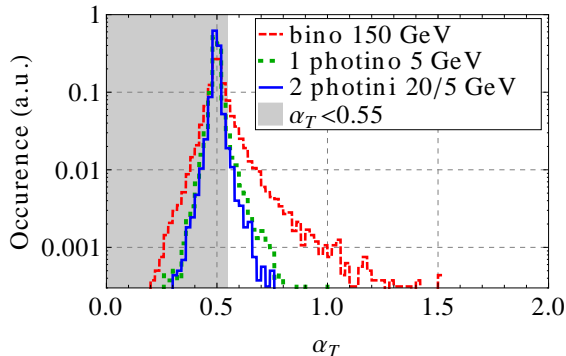


Figure 2. The histogram of the experimental α_T variable for the simplified model of 750 GeV gluino and a 150 GeV bino; the signal region is $\alpha_T \geq 0.55$ [15]. The three curves show the α_T distribution for spectra in which the bino is stable (red, dashed), the bino decays to a 5 GeV photino by Z emission (green, dotted), and the bino dominantly cascades through two photini of 20 GeV and 5 GeV by double Z emission (blue, solid).

model files for supersymmetric spectra [53]. We add n photini of mass m_i , each with kinetic mixing $\epsilon_i = \mathcal{O}(0.1)$ with the bino and diagonalize the $(4 + n) \times (4 + n)$ neutralino mass matrix at tree level to find the neutralino mass eigenstates.

For the hard SUSY processes, we simulate LHC events at $\sqrt{s} = 7$ TeV for the leading squark-squark, squark-gluino and gluino-gluino production channels using `MadGraph5 v1.4.03` [54], compute NLO cross-sections for the processes in `Prospino v2.1` [55], and scan over the two-dimensional parameter spaces in the three types of spectra above. We differentiate between the three cases in implementing cascade decays of the squarks and gluinos in `Pythia v6.426` [56] to produce parton-level event samples with the bino as the LSP (“bino samples”). We use the bino samples to validate our analysis and ensure that the limits we set on photini spectra are consistent with experimental limits up to acceptable simulation uncertainties.

In the case of squark-gluino-bino and gluino-bino simplified models, we simulate the “photini samples” by adding an extra step in the cascade with the LOSP (the LSP in the “bino samples”) decaying via Z or higgs emission, with a higgs mass of 125 GeV as suggested by recent experiments [57, 58]. To generate the photini samples in the cMSSM, we run `Pythia` directly on the cMSSM bino samples with bino decays to photini through Z and higgs bosons; we calculate the Z versus higgs boson emission rates in `Madgraph` with photini UFO model file using a higgs mass obtained from `SOFTSUSY`.⁷

Finally, in order to account for basic detector effects, we use the simplified detector simulator `PGS v120404` [59] (as part of the `Pythia-PGS v2.1.16` implementation in `Madgraph5`) with its default LHC settings and lepton isolation.

3.2 Sensitivity of hadronic searches

In order to evaluate the impact of the missing energy spectrum shifts demonstrated above, we perform a detailed analysis of experimental limits and how search efficiencies change with photini added to the spectrum. We focus on LHC searches; for the range of sparticle masses we consider ($m_{1/2} > 250$ GeV or $m_{\tilde{g}} > 400$), Tevatron and LEP searches provide no relevant limits.

⁷Note that this fixes the higgs mass to be somewhat lighter than the recent tantalizing hints of the particle at a mass of ~ 125 GeV. However, this small change would not significantly alter our results.

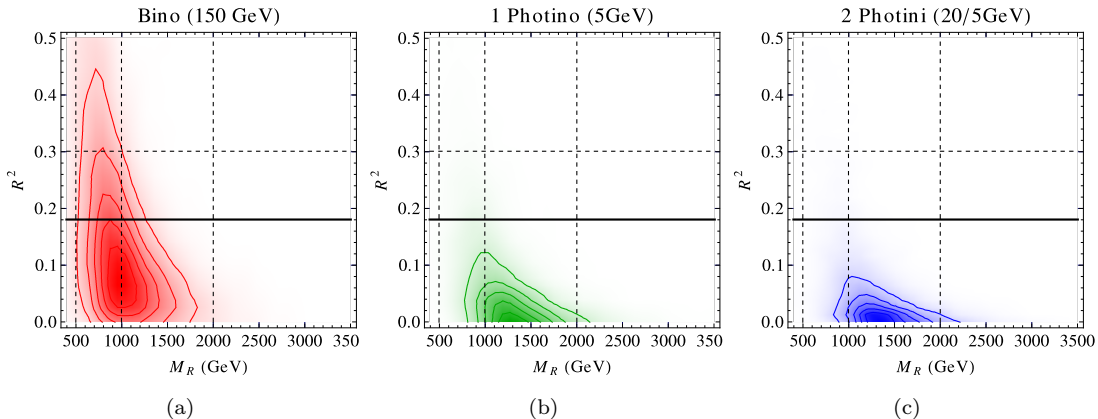


Figure 3. Razor variables density plot excluding all other selection cuts for the simplified model of 750 GeV gluino and a 150 GeV bino. The three plots concern spectra in which (a) the bino is stable; (b) the bino decays to a 5 GeV photino by Z emission; (c) the bino dominantly cascades through two photini of 20 GeV and 5 GeV by double Z emission. The six signal regions from the CMS analysis [16] correspond to the six regions outlined by the grid lines above the bold black line (i.e. $R^2 > 0.18$ and $M_R > 500$ GeV); the SUSY signal in these regions is decimated if the bino can decay to one or more photini.

First, we consider additional observables that have been defined by the CMS collaboration in order to enhance signal sensitivity, in particular α_T (Figure 2) and razor variables (Figure 3) [15, 16]. Even though these analyses are carefully optimized to search for SUSY signals, they still fundamentally rely on missing energy as a handle on the event, and are thus less effective in the presence of photini. Both α_T and the razor variable R are defined as ratios of energies in the event in order to maximize the signal to background ratio of SUSY versus Standard Model events (see Appendix A for details). We see that adding one photino to the decay chain makes the events more Standard-Model-like by diffusing the missing energy in the event (red versus green curves in Figures 2, 3). Adding a second photino to the cascade reduces the efficiency in the signal regions further.

To quantify the impact of signal reduction described above, we impose selection criteria that mimic those of the experimental LHC searches on the Monte Carlo samples. For simplicity, we include only the leading selection cuts for the experimental searches. In Appendix A, we present our exact event selection criteria for each of the relevant hadronic searches on our PGS samples, which already account for some detector efficiencies and lepton isolation cuts.

To set exclusion limits, we use the published expected and observed event counts in each experimental search region. We convolve the Poisson statistical errors with Gaussian systematics using [60]; for searches (α_T) without published errors, we estimate the systematic error to be 30%. For the simplified model search we also use a varying error on the efficiency in the gluino-bino plane as published in the 36 pb^{-1} results [61]. Despite our course-grained analysis, we find that our Monte Carlo sensitivities for cMSSM and simplified spectra (with a bino as the LSP) match well with those of CMS and ATLAS (Figures 5 and 6).

We first consider the exclusions from the ATLAS jets+ \cancel{E}_T searches in Figure 4 with the 1.04 fb^{-1} [62, 63] and 4.7 fb^{-1} [18] analyses. The ATLAS analysis is presented for a simplified model of gluino and light-generation squarks decaying to a LSP. The 1.04 fb^{-1} analysis includes LSP masses of 0, 195, and 395 GeV, while the 4.7 fb^{-1} analysis only includes direct limits on a massless LSP. Since in our scenario the bino-like neutralino is the LOSP and decays to photini, we consider the case of 195 GeV

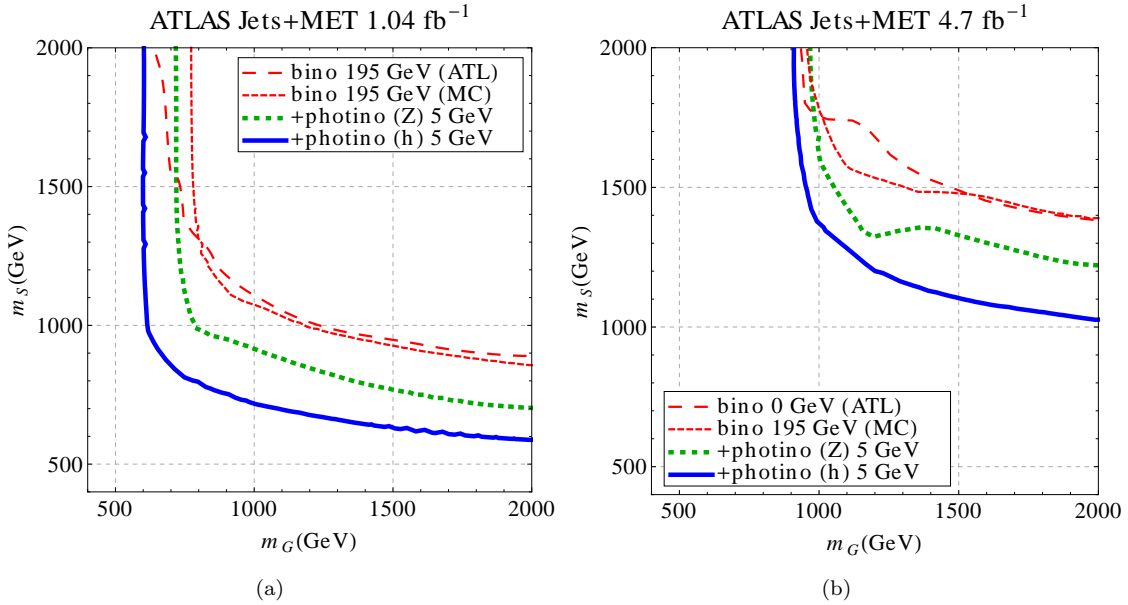


Figure 4. Allowed parameter space of the gluino-squark-bino simplified model for (a) the ATLAS 2-4 jets+ \cancel{E}_T search at 1.04 fb^{-1} , and (b) the ATLAS 2-6 jets+ \cancel{E}_T search at 4.7 fb^{-1} . The red large-dashed and small-dashed lines are the 95% exclusion limits from the ATLAS experiment and from our simulation matching, respectively. The green dotted curves are exclusion limits based on our scan of spectra with a bino LOSP decaying to a single photino through a Z boson, while the blue solid curves are the analogous limits for the bino decaying via a higgs.

LSP for comparison. In the exclusion limits published by ATLAS, there is very little distinction between the massless and 195 GeV LSP for the high mass gluino-squark region, and we find excellent agreement with our analysis and the experimental exclusion curve with both sets of data. In the case of the 1.04 fb^{-1} search (Fig. 4(a)) we rescaled both signal acceptances by 70% to match the experimental result; the discrepancy is due to looser acceptance requirements on jets in our analysis (Appendix A). In the 4.7 fb^{-1} search (Fig. 4(b)) the only slight discrepancy between our analysis and experiment is in the signal region with the highest m_{eff} cut. The relative branching ratios for bino decays through the higgs or the Z depend on the details of the neutralino mixing matrix; for simplicity we consider the two limits $\text{Br}(\tilde{N}_1 \rightarrow Z + \tilde{N}_5) = 1$ and $\text{Br}(\tilde{N}_1 \rightarrow h + \tilde{N}_5) = 1$ in the context of the simplified models. We observe a significant reduction in the limit on the squark mass, and a more modest reduction for the gluino mass. We also consider the ATLAS multijet analysis [64] in this scenario; however, especially as the gluino limits are not significantly eroded, the limit from the 6-9 jet search is subleading and we do not present it here.

We present the effect of photini on the CMS α_T and CMS jets+ \cancel{E}_T searches for the gluino-bino simplified models in Figure 5. To best approximate the experimental procedure, for α_T searches we use a combination of the 6 highest H_T signal regions, and for the jets+ \cancel{E}_T search we use the best limit at each point in parameter space. For heavier LOSPs some of the efficiencies in this very simple model increase as a result of the extra step in the decay chain. This is due to two factors: first, in the case of the very squeezed spectrum of gluino and bino within 300 GeV, the gluino decay through off-shell squarks produces soft jets, resulting in low hadronic energy. If the bino then decays hadronically to a

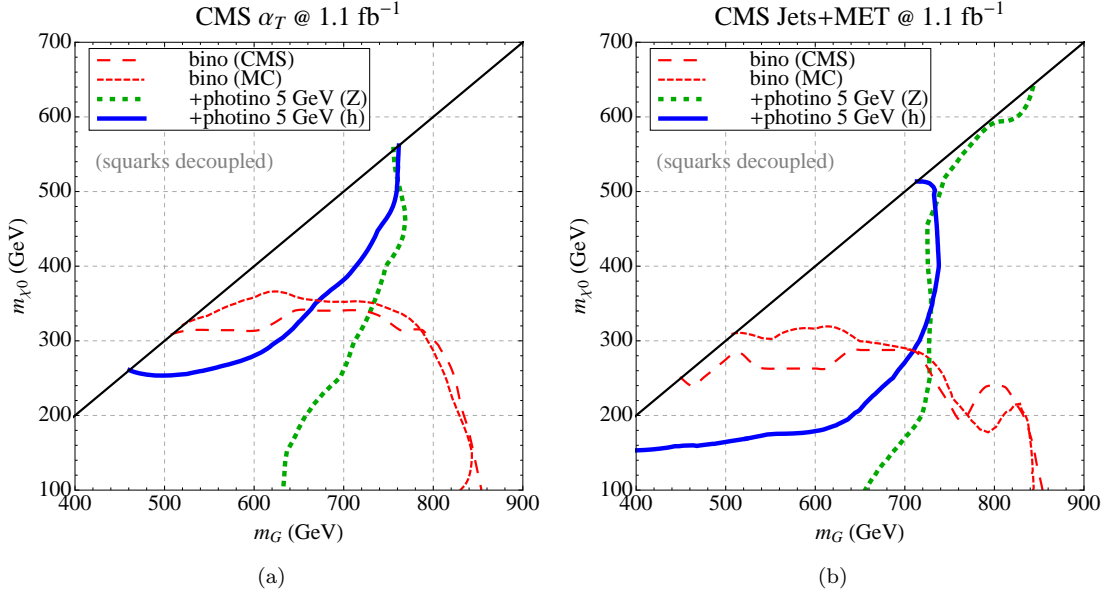


Figure 5. Allowed parameter space after (a) CMS α_T and (b) CMS jets+ \cancel{E}_T searches at 1 fb^{-1} in the simplified model gluino-bino mass plane. The red large-dashed and small-dashed lines are the experimental limit and our simulation matching, respectively. The green dotted and blue solid lines are the limits corresponding to bino decay via Z -emission and higgs emission to a photino. Above the black line is the kinematic limit of the experimental reach due to very high systematic uncertainty for small gluino-bino mass splittings; the excluded region is between the diagonal black line and the blue (solid) and green (dotted) photino lines. Below LOSP masses of 200 GeV, the higgs decay channel exclusion is not reliable since large squeezing leads to soft jets and small missing energy, causing high sensitivity to the precise implementation of the cuts.

much lighter photino, there is much more visible energy in the event. Second, the gluinos in the hard collision are produced in approximately opposite azimuthal directions, so if the mass splitting with the bino is small, the bino transverse momenta are also nearly antiparallel and much of the transverse missing energy in the event cancels. However, if the bino now decays to a Z and photino, the photino momenta from the two decay chains become uncorrelated and do not in general cancel, leading to more missing energy.

On the other hand, with a photino added to the spectrum and a light bino LOSP, limits on the gluino mass decrease by 200 GeV or more in Z decays and reach the kinematic limit in higgs decays. For the higgs decay, the CMS high H_T signal region sets the tightest bounds, as missing energy is squeezed out especially for bino masses near 150 GeV, close to the higgs at 125 GeV (Fig 5(b)). In the case of the α_T analysis, the search efficiency for low bino-higgs mass splitting is even lower at $\mathcal{O}(10^{-3})$ - $\mathcal{O}(10^{-4})$ as the low missing energy leads to α_T values of 0.5 or less, below the cut for the signal region (Fig 5(a)). Below LOSP masses of 200 GeV, the higgs decay channel exclusion is not reliable since large squeezing leads to soft jets and small missing energy, causing high sensitivity to the precise implementation of the cuts.

In Figure 6, we show how the reach for the hadronic searches (a) CMS α_T and (b) CMS jets+ \cancel{E}_T is altered by photini in a cMSSM model framework. For the α_T search (Figure 6(a)), the exclusion limit comes mainly from the highest H_T signal region, and we observe accurate agreement between

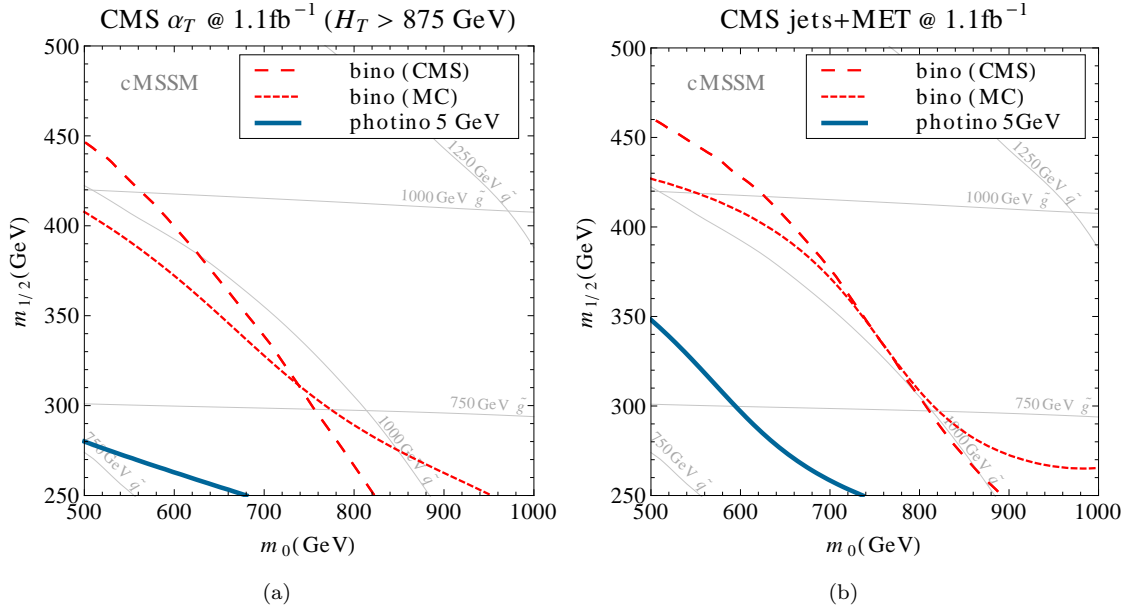


Figure 6. Allowed cMSSM parameter space for (a) the CMS α_T search, and (b) the CMS jets+ \cancel{E}_T search. The red curves with large dashes are the 95% exclusion limits on the cMSSM parameter space, as set by the LHC experiments. The red dashed curves are the interpolated exclusion limits based on our scan of cMSSM spectra with a bino LSP, while the teal solid curves are the analogous limits for the cMSSM spectra with an additional photino of 5 GeV.

the experimental exclusion curve (large dashes) and the matched exclusion curve on our Monte Carlo data with a bino LSP (small dashes). The analogous limit on spectra with photini is represented by the dashed red curve. Similarly, in Figure 6(b) we show the same curves for the CMS jets+ \cancel{E}_T , where teal solid lines represent the limits set by the “high \cancel{H}_T ” signal region (see Appendix A for a more details on the selection cuts). For both searches⁸ (α_T and jets+ \cancel{E}_T), we rescaled our Monte Carlo signals for both the bino and photino samples by a global factor of 75% to match the published experimental limits for cMSSM spectra. This rescaling is necessary due to the treatment of leptons, for which the CMS experiment generally has looser isolation cuts than PGS. Since both of the CMS searches considered here veto on leptons in the event, a slight overestimate of the signal is to be expected due to the reduced number of leptons passing isolation cuts. Note also the slight differences in shape between our exclusion curves for the bino samples and the experimental limit curves; this is due to the higher lepton multiplicity in the region of parameter space with high m_0 and low $m_{1/2}$.⁹ The sensitivity of the high \cancel{H}_T signal region is much reduced for the photino samples. In fact, for these samples the high H_T channel is the most constraining, although the limits are also reduced for this signal region.

⁸We do not present our cMSSM exclusion limit analysis for the $\sim 5 \text{ fb}^{-1}$ CMS razor and ATLAS 2-6 jets+ \cancel{E}_T SUSY searches. For the CMS razor search, our matching to the experimental limits was poor due to complex statistical methods in the CMS analysis, and we found the ATLAS jets+ \cancel{E}_T limits to be more usefully interpreted in the simplified model framework.

⁹As a modest validation, this rescaling is not necessary to achieve good agreement for the simplified models, where the production of leptons is decoupled by construction.

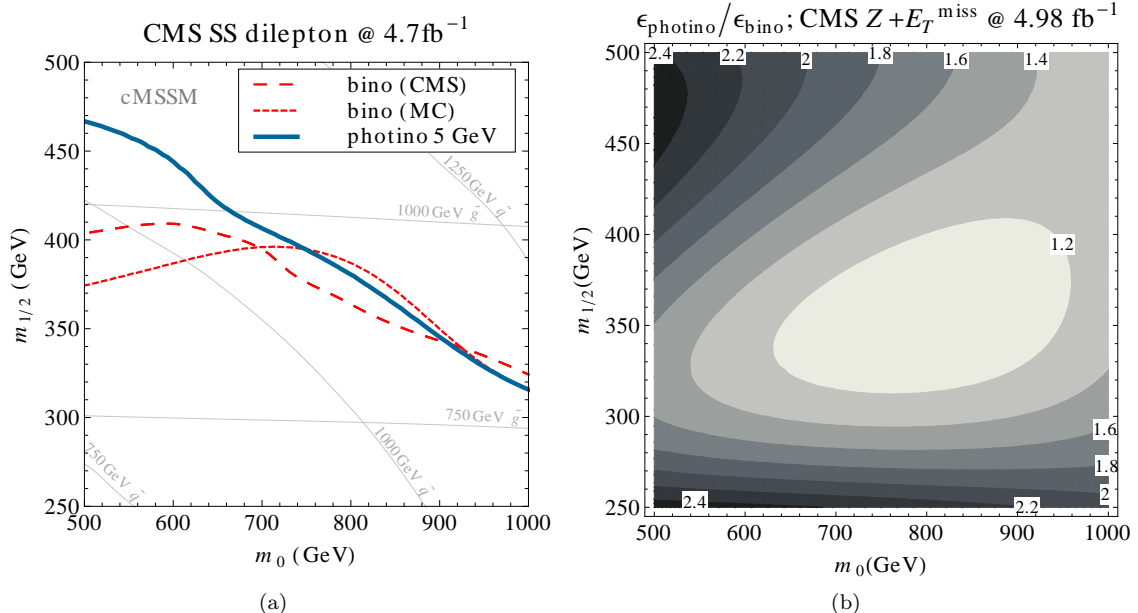


Figure 7. (a) The 95% CL exclusion limit on the cMSSM parameter space set by the CMS SS dilepton search using the most constraining signal region. The red large-dashed curve is the limit set by CMS, the red dashed curve is the 95% CL exclusion limit on our Monte Carlo data with the bino as the LSP, and the teal solid curve is the analogous curve with photino as the LSP. (b) Contours of the ratio of the selection efficiency with ($\epsilon_{\text{photino}}$) and without (ϵ_{bino}) a 5 GeV photino in the cMSSM spectrum, for the $Z+\text{jets}+\cancel{E}_T$ search using the JZB variable.

4 Finding SUSY

In the previous section, we demonstrated how extending a supersymmetric spectrum by one or more photini can significantly alter the nature of experimental signatures and reduce the reach of the hadronic LHC searches, which currently set the most stringent limits on SUSY production. However, the decays of the LOSP (taken here to be a mostly-bino neutralino) to photini via Z and/or higgs bosons can lead to signatures in other channels, most notably those involving same-sign (SS) leptons, opposite-sign (OS) leptons, and bottom quarks, in addition to some missing energy. The additional contributions to these signal channels may improve their effectiveness in setting limits, and indeed may render them the most promising channels for discovery. We investigate the reach of leptonic SUSY searches at the LHC in two separate frameworks, namely the cMSSM and the gluino-squark-bino simplified model of Section 3.1.

To study the sensitivity of leptonic searches in the cMSSM framework, we focus on the dedicated CMS searches for SS dileptons and \cancel{E}_T [65, 66], and leptonically-decaying Z bosons and \cancel{E}_T [67]. We perform simple versions of the CMS SS dilepton search at 4.7 fb^{-1} and the $Z+\text{jets}+\cancel{E}_T$ SUSY search at 4.98 fb^{-1} on our cMSSM Monte Carlo samples to estimate the leptonic detection reach for our model. The SS dilepton search looks for sufficiently hard pairs of ee , $e\mu$ or $\mu\mu$ along with a minimum \cancel{E}_T requirement and a veto on opposite-sign, same-flavor lepton pairs that reconstruct the Z . The $Z+\text{jets}+\cancel{E}_T$ search selects events based on jet energy, lepton energy, and jet- Z balance (dubbed JZB) with cuts similar to those listed in [67]. The JZB variable can be thought of as a measure of \cancel{E}_T with sign information; under- or over-measurement of the jet energy generally leads to negative or positive

JZB , respectively. Since jet energy is more likely to be under-measured in a detector and SUSY events typically have signatures with positive JZB , cutting on events with the requirement $JZB > 150$ GeV is an effective way to achieve good signal versus background separation. More detailed criteria for both searches are listed in Appendix A.

In Figure 7(a), we show the limits on the cMSSM set by the CMS SS dilepton search in the most constraining signal region (SR #4, see Appendix A). To account for the discrepancy of lepton detection efficiencies between our PGS simulation and experiment, we rescale our efficiencies by 80%. We can see that the detection reach is largely unaffected by photini despite the \cancel{E}_T reduction and a higher occurrence of Z vetos from OSSF leptons, as there is also a higher multiplicity of SS lepton pairs. As such, the SS dilepton search remains an effective means of looking for SUSY with photini cascades, and in many cases may set the most stringent limits on the spectrum. This raises the tantalizing possibility of first discovering SUSY in a leptonic search.

In Figure 7(b), we show a contour plot of the ratio of selection efficiencies for the Z +jets+ \cancel{E}_T search with and without a photino of 5 GeV. We present selection efficiencies only because CMS has not yet released limits on the full cMSSM parameter space in this search. However, any systematic errors in our treatment of leptons will largely cancel out in a ratio of efficiencies, and suffices to paint a qualitative picture of the change in detection reach in the presence of photini. We observe that the sensitivity of the search increases by a factor of 1.2 to 2.4, depending on the spectrum and the signal region. The contours shown are for the signal region with the tightest JZB requirements; for other signal regions with lower JZB cuts, the ratio of bino to photino efficiencies changes by up to 10%. Unsurprisingly, this suggests an increased sensitivity of the Z +jets+ \cancel{E}_T search to cascade decays involving light photini due to the additional on-shell Z bosons.

There are other searches that may prove to be sensitive to detecting extended SUSY cascades with photini, though for various reasons they are typically somewhat less effective than SS dileptons when applied to the cMSSM. The multilepton searches [68] are not particularly sensitive to OSSF pairs of leptons with invariant mass near the Z mass, but may prove constraining when there is additional leptonic activity in the decay chain or when decays proceed predominantly through the higgs. Note that the multilepton search becomes more effective when the mass splitting between the LOSP and the lightest photino is small and the Z is far off-shell, but in this case the \cancel{E}_T distribution is not significantly altered and standard hadronic SUSY searches provide stronger limits. Ancillary searches such as opposite-sign dilepton plus \cancel{E}_T [69] mainly look for a kinematic edge of OSSF leptons outside of the di-lepton invariant mass window of the Z boson, rendering these studies less effective for constraining the case at hand. Searches involving bottom quarks [70–72] may become sensitive especially when the dominant decay from the bino to a photini occurs through emission of a light higgs boson, though for these decays the \cancel{E}_T signal is significantly reduced.

For completeness, we also consider the implications of leptonic searches for our simplified models, though in this case the decoupling of sleptons and electroweakinos has an important impact on the relative sensitivity of various searches. Focusing on the squark-gluino-bino simplified model, we perform analyses similar to the CMS same-sign dilepton search (with 5 fb^{-1} , [65]) and ATLAS opposite-sign dilepton search (with 1 fb^{-1} , [73]), and compare to the reach of the hadronic ATLAS jets searches for 1 fb^{-1} and 5 fb^{-1} considered in Section 3.2. A simplified spectrum in which only squarks, gluinos, and binos are accessible at LHC energies does not yield many leptons by construction, so here we only consider the case of the bino decaying to a photino by Z or higgs boson emission (and not the case of a stable bino). There is an additional uncertainty in our results for these two leptonic searches from our treatment of leptons; in this simplified model framework we could not validate our exclusion curves against published experimental exclusion curves with the bino as the LSP (as opposed to the cMSSM

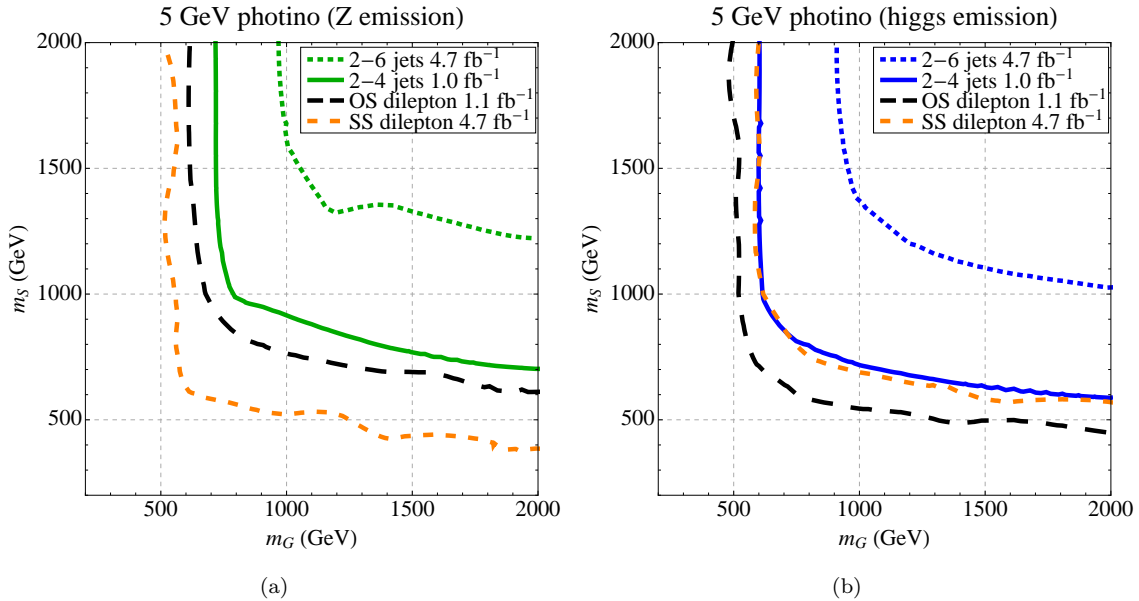


Figure 8. Exclusion limits on the squark-guino-bino simplified model in the presence of a 5 GeV photino in the case the LOSP decays to the photino via (a) a Z boson or via (b) a higgs boson. We take only the first two squark generations light and the remaining sparticles decoupled at 3.5 TeV. We compare the reach of the ATLAS 2-6 jets and \cancel{E}_T search for (a) Z emission (dotted, green curve) and (b) higgs emission (dotted, blue curve), the ATLAS 2-4 jets and \cancel{E}_T search for (a) Z emission (solid, green curve) and (b) higgs emission (solid, blue curve), to two leptonic searches: OS dileptons (black, large dashed), and SS dileptons (orange, small dashed). The OS dilepton search has a larger missing transverse momentum cut, leading to a weaker limit on higgs emission in (b) compared to Z emission in (a).

framework, e.g. see the two red curves in Figure 7(a)). We implement a rescaling of the efficiencies by 80% as in the cMSSM scenario to account for experimental leptonic efficiencies.

As the photini cascades inject additional leptons into the events through Z or higgs boson emission, the leptonic searches become competitive with jets and missing energy searches for these simplified models. In Figure 8 we demonstrate that even in the simplified model context, the opposite-sign lepton with missing energy searches are comparable to the 2-4 jets and \cancel{E}_T search with the same integrated luminosity. In the case of a more complete supersymmetric spectrum, we expect the leptonic searches to be even more effective, as the decays to photini will be one of several sources of leptons (in addition to slepton and stop decays, for instance). This is particularly true in the case of SS dilepton searches, which are very effective for the cMSSM (see Figure 7(a)) but less so for simplified models; to pass the SS dilepton cuts as shown in Figure 8, both Z 's or higgses in the event have to decay leptonically, reducing the efficiency by small branching ratios. Other leptonic searches such as CMS multileptons [68] or ATLAS trileptons [74] could be very sensitive to photini produced via higgs decays in the Z -veto signal regions. However, we note that the current ATLAS trilepton search also vetoes on b-tags, which nearly eliminates the signal. This underlines the importance of leptonic searches with 0, 1, or 2 b-tags in order to capture higgs decays in supersymmetric decay chains.

The sensitivity of the searches considered here highlights the fact that the presence of additional gauge fermions mixing with the bino may mitigate limits from the hadronic SUSY searches with the greatest reach, but does not extinguish SUSY signals entirely. Indeed, it suggests that in many cases

the first SUSY signals may arise in search channels involving Z 's, leptons, or other supplementary tags whose sensitivity is unaltered or improved by the presence of photini. Finally, it would be especially interesting to probe the sensitivity of proposed SUSY searches that rely on lepton and jet multiplicity, rather than \cancel{E}_T [75], since extended cascade decays involving photini are likely to enhance the relevant SUSY signal.

5 Conclusions

In this work we have studied the phenomenology of photini – additional light abelian gauge fermions – on SUSY searches at the LHC. The existence of these light fermionic degrees of freedom is natural in the context of string compactifications, though the phenomenology is common to any models in which extra neutral fermions mix with MSSM neutralinos. We performed a detailed analysis of the impact of SUSY spectra with photini on current hadronic searches; the limits set on squark and gluino masses by the most constraining searches at both ATLAS and CMS are reduced dramatically. The reduction persists for spectra in two simplified models as well as the cMSSM, with the latter case providing a reasonable sample of longer cascade decays.

In particular, for a simplified model consisting of a gluino, light-flavor squarks, and a 195 GeV bino LOSP, bounds on the squark masses are relaxed to as low as 1 TeV from the current best limit of 1.4 TeV squarks for a 2 TeV gluino. While “squeezed” spectra with a bino-gluino splitting below 300 GeV actually become more constrained in the presence of photini due to kinematics, the limit reduction is dramatic for natural LOSP masses of the same order as the higgs mass. In fact, in the limit in which all sparticles are decoupled except for the gluino and LOSP (motivated by e.g. split supersymmetry), the leading hadronic SUSY searches at CMS cannot exclude any spectrum with gluinos heavier than 400 GeV and a bino of mass $m_{\tilde{N}_1} \lesssim 160$ GeV that dominantly decays to the lightest photino through 125 GeV higgs emission. The CMS α_T variable in particular is only weakly sensitive to photini events with small missing energy. More standard hadronic and \cancel{E}_T searches at ATLAS and CMS are less compromised, but set reduced limits up to the kinematic edge of a LOSP nearly degenerate in mass with the higgs.

We emphasize that we have only considered one limit of photino parameter space, in which photini couplings are moderate and decays proceed through on-shell Standard Model fields. There are a variety of other parametric regions that may reduce the sensitivity of SUSY searches. In particular, as the photini mixing is reduced, decays involving photini may involve displaced vertices. Depending on the decay length, these cascades may evade searches that depend on impact parameter and track quality – a sort of R -preserving version of displaced supersymmetry [25].

In general, supersymmetry concealed by photini or similar light degrees of freedom will not be impossible to discover at the LHC. Although the sensitivity of frontier searches relying on jets and missing energy may be significantly eroded, it will not be entirely compromised. Ancillary searches with sensitivity to Z 's or additional leptons should provide compensatory coverage, although their current reach is not as great. For the most part, exceptionally sophisticated new techniques will not be required, but rather the persistent pursuit of a wide range of complementary SUSY search strategies. But by eroding the sensitivity of the SUSY searches with greatest reach, the presence of photini in decay chains may render natural supersymmetric spectra more compatible with current LHC data and increase the prospects of discovering supersymmetry in novel channels.

Acknowledgments

We thank Asimina Arvanitaki, Erik Devetak, Savas Dimopoulos, Eleanor Dobson, Sergei Dubovsky, and John March-Russell for useful conversations, and Josh Ruderman and Prashant Saraswat for helpful comments on the manuscript. We are especially grateful to Eder Izaguirre and Jay Wacker for providing Madgraph simplified model data, and to Benjamin Fuks for support regarding the Feynrules program. This work was supported in part by ERC grant BSMOXFORD no. 228169. MB is supported in part by the NSF Graduate Research Fellowship under Grant No. DGE-1147470. NC is supported by NSF grant PHY-0907744, DOE grant DE-FG02-96ER40959, and the Institute for Advanced Study, and acknowledges hospitality from the Stanford Institute for Theoretical Physics where parts of this work were completed.

A Selection cuts

1. CMS α_T search (1.1 fb⁻¹) [15]:

- jet requirements of $E_T > 50$ GeV and pseudorapidity $|\eta| < 3$
- $H_T > 275$ GeV, where H_T is defined as the scalar sum of the jet E_T 's; we combine limits from the following 6 H_T bins throughout our paper: (375-475, 475-575, 575-675, 675-775, 775-875, 875+);¹⁰
- lepton veto (no electron or muon with $p_T > 10$ GeV);
- central leading jet (the hardest jet needs to have $|\eta| < 2.5$;
- two hard jets (the hardest two jets both need to have $E_T > 100$ GeV);
- $R_{\text{miss}} \equiv \frac{\cancel{H}_T}{\cancel{E}_T} < 1.25$, where the \cancel{H}_T is a jet-based measure of missing energy (namely the E_T of the vectorial sum of all jets) and \cancel{E}_T is the missing transverse energy measured at the calorimeter level
- $\alpha_T \equiv \frac{E_T^{j_2}}{M_T} > 0.55$, where M_T is defined as the total transverse mass of all jets, and $E_T^{j_2}$ is the transverse energy of the sub-leading jet if the jet multiplicity $n = 2$ (for $n > 2$, two pseudojets are first formed according to [15]).

2. CMS razor variables search (4.4 fb⁻¹) [16]:¹¹

- jets need to have $E_T > 60$ GeV and $|\eta| < 3$;
- $1000 \text{ GeV} < M_R < 3500 \text{ GeV}$ and $0.18 < R^2 < 0.5$, where $M_R \equiv \sqrt{(E^{j_1} + E^{j_2})^2 - (p_z^{j_1} + p_z^{j_2})^2}$, $M_T^R \equiv \sqrt{\frac{\cancel{E}_T(p_T^{j_1} + p_T^{j_2}) - \vec{\cancel{E}}_T \cdot (\vec{p}_T^{j_1} + \vec{p}_T^{j_2})}{2}}$, $R \equiv \frac{M_T^R}{M_R}$, and j_1/j_2 are two ‘‘megajets’’ defined according to [16].

3. CMS jets+ \cancel{E}_T search (1.1 fb⁻¹)[17]:

- ≥ 3 jets with $p_T > 50$ GeV and $|\eta| < 2.5$;
- lepton veto (no electron or muon with $p_T > 8$ GeV and $|\eta| < 2.1$);

¹⁰In addition, [15] defines two lower H_T bins, (275-325) and (325-375) but these set no limits for the spectra considered in our paper.

¹¹We implement these cuts for Fig. 3 to illustrate the shifts in the M_R and R^2 variables. The full search contains a more baseline requirements, such as a veto on leptons.

- $H_T > 350$ GeV, where H_T is calculated based on jets with $p_T > 50$ GeV and $|\eta| < 5$;
 - $\cancel{H}_T > 200$ GeV, where \cancel{H}_T is calculated based on jets with $p_T > 30$ GeV and $|\eta| < 5$;
 - \cancel{H}_T four-momentum isolation from the three leading jets in the $eta - \phi$ plane (by a distance of 0.5 for the two leading jets, 0.3 for the third-hardest jet)
 - three signal regions: “high H_T ” ($H_T > 800$ GeV), “medium H_T and \cancel{H}_T ” ($H_T > 500$ GeV, $\cancel{H}_T > 350$ GeV), and “high \cancel{H}_T ” ($\cancel{H}_T > 500$ GeV) as described in [17].
4. ATLAS 2-4 jets+ \cancel{E}_T search (1.04 fb^{-1}) [62]:
- $\cancel{E}_T > 130$ GeV
 - Leading jet $p_T > 130$ GeV, other jets $p_T > 80$ GeV, for 5 or more $p_T > 40$ GeV,
 - m_{eff} cuts between 500 and 1100 GeV where $m_{\text{eff}} = \cancel{E}_T + \sum_{\text{jets}} |p_T|$,
 - lepton veto (no electron or muon with $p_T > 20$ GeV),
 - $\cancel{E}_T/m_{\text{eff}}$ cuts between 0.2 and 0.3,
 - Five signal regions based on number of jets, m_{eff} , and $\cancel{E}_T/m_{\text{eff}}$ as in [62]. The limit on signal is set by the most constraining region at each point in parameter space.
5. ATLAS 2-6 jets+ \cancel{E}_T search (4.7 fb^{-1}) [18]
- $\cancel{E}_T > 160$ GeV;
 - leading jet $p_T > 130$ GeV, other jets $p_T > 60$ GeV, for 5 or more $p_T > 40$ GeV;
 - m_{eff} cuts between 900 and 1900 GeV where $m_{\text{eff}} = \cancel{E}_T + \sum_{\text{jets}} |p_T|$;
 - lepton veto (no electron or muon with $p_T > 20$ GeV);
 - $\cancel{E}_T/m_{\text{eff}}$ cuts between 0.15 and 0.4;
 - 11 signal regions based on number of jets, m_{eff} , and $\cancel{E}_T/m_{\text{eff}}$ as in [18]. The limit on signal is set by the most constraining region at each point in parameter space.
6. CMS same sign (SS) dilepton search (4.7 fb^{-1}) [65, 66], high- p_T lepton baseline, signal region #4
- ≥ 2 jets in event, each with $p_T > 40$ GeV and $|\eta| < 2.5$;
 - baseline lepton requirements of $p_T > 5$ GeV for muons, $p_T > 10$ GeV for electrons, $|\eta| < 2.4$ for both flavors;
 - veto on opposite sign same flavor (OSSF) pairs that reconstruct the Z (i.e. $76 \text{ GeV} < m_{ll} < 106 \text{ GeV}$);
 - at least one same-sign (SS) dilepton pair of type $e\mu$, ee or $\mu\mu$, each with $p_T > 10$ GeV;
 - the leading lepton in the event (not necessarily out of the dilepton pair) has $p_T > 20$ GeV;
 - $\cancel{E}_T > 100$ GeV.
7. JZB +jets+ \cancel{E}_T [67]
- ≥ 3 central jets with $p_T > 50$ GeV and $|\eta| < 2.5$;
 - at least one pair of OSSF leptons with $p_T > 20$ GeV which reconstruct the Z boson to mass to within 20 GeV ($|m_{l+l-} - m_Z| < 20 \text{ GeV}$);

- the hardest isolated OSSF lepton pair needs to have $JZB > 150$ GeV, where JZB is defined as

$$JZB \equiv \left| \sum_{\text{jets}} \vec{p}_T \right| - \left| \vec{p}_T^{(Z)} \right| \quad (\text{A.1})$$

and serves as a measure of the \cancel{E}_T in the event.

- ATLAS dilepton and missing transverse momentum search (1 fb^{-1}) [73], “OS-inc” signal region
 - $E_T^{\text{miss}} > 250$ GeV, where E_T^{miss} is the magnitude of the vector sum of the p_T of jets with $p_T > 20$ GeV and signal leptons;
 - baseline lepton requirements of $p_T > 20$ GeV, $|\eta| < 2.47$ for electrons, $p_T > 10$ GeV, $|\eta| < 2.4$ for muons;
 - isolation requirements on leptons: energy within a cone of $\Delta R < 0.2$ is less than 10% of the p_T for electrons or 1.8 GeV for muons;
 - exactly two leptons as defined by the above momentum and isolation cuts in the event;
 - invariant dilepton mass $m_{ll} > 12$ GeV to suppress low-mass resonances;
 - one opposite-sign (OS) dilepton pair of type $e\mu$, ee or $\mu\mu$;
 - the leading lepton in the event has $p_T > 20$ GeV for a muon or $p_T > 25$ GeV for an electron.

References

- [1] **ATLAS** Collaboration, G. Aad *et al.*, *Combined search for the Standard Model Higgs boson using up to 4.9 fb⁻¹ of pp collision data at sqrt(s) = 7 TeV with the ATLAS detector at the LHC*, *Phys.Lett.* **B710** (2012) 49–66, [[arXiv:1202.1408](#)].
- [2] **CMS** Collaboration, S. Chatrchyan *et al.*, *Combined results of searches for the standard model Higgs boson in pp collisions at sqrt(s) = 7 TeV*, *Phys.Lett.* **B710** (2012) 26–48, [[arXiv:1202.1488](#)].
- [3] N. Arkani-Hamed and S. Dimopoulos, *Supersymmetric unification without low energy supersymmetry and signatures for fine-tuning at the LHC*, *JHEP* **0506** (2005) 073, [[hep-th/0405159](#)].
- [4] G. Giudice and A. Romanino, *Split supersymmetry*, *Nucl.Phys.* **B699** (2004) 65–89, [[hep-ph/0406088](#)].
- [5] S. Dimopoulos and G. Giudice, *Naturalness constraints in supersymmetric theories with nonuniversal soft terms*, *Phys.Lett.* **B357** (1995) 573–578, [[hep-ph/9507282](#)].
- [6] R. Essig, E. Izaguirre, J. Kaplan, and J. G. Wacker, *Heavy Flavor Simplified Models at the LHC*, *JHEP* **1201** (2012) 074, [[arXiv:1110.6443](#)].
- [7] Y. Kats, P. Meade, M. Reece, and D. Shih, *The Status of GMSB After 1/fb at the LHC*, [[arXiv:1110.6444](#)].
- [8] M. Papucci, J. T. Ruderman, and A. Weiler, *Natural SUSY Endures*, [[arXiv:1110.6926](#)].
- [9] C. Brust, A. Katz, S. Lawrence, and R. Sundrum, *SUSY, the Third Generation and the LHC*, [[arXiv:1110.6670](#)].
- [10] G. F. Giudice, M. Nardecchia, and A. Romanino, *Hierarchical Soft Terms and Flavor Physics*, *Nucl.Phys.* **B813** (2009) 156–173, [[arXiv:0812.3610](#)].
- [11] N. Craig, D. Green, and A. Katz, *(De)Constructing a Natural and Flavorful Supersymmetric Standard Model*, *JHEP* **1107** (2011) 045, [[arXiv:1103.3708](#)].

- [12] R. Barbieri, G. Isidori, J. Jones-Perez, P. Lodone, and D. M. Straub, *$U(2)$ and Minimal Flavour Violation in Supersymmetry*, *Eur.Phys.J.* **C71** (2011) 1725, [[arXiv:1105.2296](#)].
- [13] N. Craig, M. McCullough, and J. Thaler, *Flavor Mediation Delivers Natural SUSY*, [arXiv:1203.1622](#).
- [14] G. D. Kribs and A. Martin, *Supersoft Supersymmetry is Super-Safe*, [arXiv:1203.4821](#).
- [15] **CMS** Collaboration, S. Chatrchyan *et al.*, *Search for Supersymmetry at the LHC in Events with Jets and Missing Transverse Energy*, *Phys.Rev.Lett.* **107** (2011) 221804, [[arXiv:1109.2352](#)].
- [16] **CMS** Collaboration, *Search for supersymmetry with the razor variables at CMS*, .
CMS-PAS-SUS-12-005.
- [17] **CMS** Collaboration, *Search for supersymmetry in all-hadronic events with missing energy*, .
CMS-PAS-SUS-11-004.
- [18] *Search for squarks and gluinos using final states with jets and missing transverse momentum with the atlas detector in $s = 7$ tev proton-proton collisions*, Tech. Rep. ATLAS-CONF-2012-033, CERN, Geneva, Mar, 2012.
- [19] T. J. LeCompte and S. P. Martin, *Large Hadron Collider reach for supersymmetric models with compressed mass spectra*, *Phys.Rev.* **D84** (2011) 015004, [[arXiv:1105.4304](#)].
- [20] T. J. LeCompte and S. P. Martin, *Compressed supersymmetry after $1/\text{fb}$ at the Large Hadron Collider*, *Phys.Rev.* **D85** (2012) 035023, [[arXiv:1111.6897](#)].
- [21] L. M. Carpenter, D. E. Kaplan, and E.-J. Rhee, *Reduced fine-tuning in supersymmetry with R -parity violation*, *Phys.Rev.Lett.* **99** (2007) 211801, [[hep-ph/0607204](#)].
- [22] C. Csaki, Y. Grossman, and B. Heidenreich, *MFV SUSY: A Natural Theory for R -Parity Violation*, [arXiv:1111.1239](#).
- [23] H. Dreiner and T. Stefaniak, *Bounds on R -parity Violation from Resonant Slepton Production at the LHC*, [arXiv:1201.5014](#).
- [24] B. Allanach and B. Gripaios, *Hide and Seek With Natural Supersymmetry at the LHC*, [arXiv:1202.6616](#).
- [25] P. W. Graham, D. E. Kaplan, S. Rajendran, and P. Saraswat, *Displaced Supersymmetry*, [arXiv:1204.6038](#).
- [26] J. Fan, M. Reece, and J. T. Ruderman, *Stealth Supersymmetry*, [arXiv:1105.5135](#).
- [27] J. Fan, M. Reece, and J. T. Ruderman, *A Stealth Supersymmetry Sampler*, [arXiv:1201.4875](#).
- [28] A. Arvanitaki, N. Craig, S. Dimopoulos, S. Dubovsky, and J. March-Russell, *String Photini at the LHC*, *Phys.Rev.* **D81** (2010) 075018, [[arXiv:0909.5440](#)].
- [29] C. Cheung, Y. Nomura, and J. Thaler, *Goldstini*, *JHEP* **1003** (2010) 073, [[arXiv:1002.1967](#)].
- [30] C. Cheung, J. Mardon, Y. Nomura, and J. Thaler, *A Definitive Signal of Multiple Supersymmetry Breaking*, *JHEP* **1007** (2010) 035, [[arXiv:1004.4637](#)].
- [31] N. Craig, J. March-Russell, and M. McCullough, *The Goldstini Variations*, *JHEP* **1010** (2010) 095, [[arXiv:1007.1239](#)].
- [32] D. Das, U. Ellwanger, and A. M. Teixeira, *Modified Signals for Supersymmetry in the NMSSM with a Singlino-like LSP*, *JHEP* **1204** (2012) 067, [[arXiv:1202.5244](#)].
- [33] A. Ibarra, A. Ringwald, and C. Weniger, *Hidden gauginos of an unbroken $U(1)$: Cosmological constraints and phenomenological prospects*, *JCAP* **0901** (2009) 003, [[arXiv:0809.3196](#)].
- [34] P. Svrcek and E. Witten, *Axions In String Theory*, *JHEP* **0606** (2006) 051, [[hep-th/0605206](#)].

- [35] A. Arvanitaki, S. Dimopoulos, S. Dubovsky, N. Kaloper, and J. March-Russell, *String Axiverse*, *Phys.Rev.* **D81** (2010) 123530, [[arXiv:0905.4720](#)].
- [36] S. Davidson and M. E. Peskin, *Astrophysical bounds on millicharged particles in models with a paraphoton*, *Phys.Rev.* **D49** (1994) 2114–2117, [[hep-ph/9310288](#)].
- [37] S. Davidson, S. Hannestad, and G. Raffelt, *Updated bounds on millicharged particles*, *JHEP* **0005** (2000) 003, [[hep-ph/0001179](#)].
- [38] S. Dubovsky, D. Gorbunov, and G. Rubtsov, *Narrowing the window for millicharged particles by CMB anisotropy*, *JETP Lett.* **79** (2004) 1–5, [[hep-ph/0311189](#)].
- [39] A. Melchiorri, A. Polosa, and A. Strumia, *New bounds on millicharged particles from cosmology*, *Phys.Lett.* **B650** (2007) 416–420, [[hep-ph/0703144](#)].
- [40] K. R. Dienes, C. F. Kolda, and J. March-Russell, *Kinetic mixing and the supersymmetric gauge hierarchy*, *Nucl.Phys.* **B492** (1997) 104–118, [[hep-ph/9610479](#)].
- [41] B. Holdom, *Oblique electroweak corrections and an extra gauge boson*, *Phys.Lett.* **B259** (1991) 329–334.
- [42] J. F. Gunion and H. E. Haber, *TWO-BODY DECAYS OF NEUTRALINOS AND CHARGINOS*, *Phys.Rev.* **D37** (1988) 2515.
- [43] **LHC New Physics Working Group** Collaboration, D. Alves *et al.*, *Simplified Models for LHC New Physics Searches*, [arXiv:1105.2838](#).
- [44] J. Alwall, P. Schuster, and N. Toro, *Simplified Models for a First Characterization of New Physics at the LHC*, *Phys.Rev.* **D79** (2009) 075020, [[arXiv:0810.3921](#)].
- [45] G. L. Kane, C. F. Kolda, L. Roszkowski, and J. D. Wells, *Study of constrained minimal supersymmetry*, *Phys.Rev.* **D49** (1994) 6173–6210, [[hep-ph/9312272](#)].
- [46] A. H. Chamseddine, R. L. Arnowitt, and P. Nath, *Locally Supersymmetric Grand Unification*, *Phys.Rev.Lett.* **49** (1982) 970.
- [47] R. Barbieri, S. Ferrara, and C. A. Savoy, *Gauge Models with Spontaneously Broken Local Supersymmetry*, *Phys.Lett.* **B119** (1982) 343.
- [48] L. E. Ibanez, *Locally Supersymmetric SU(5) Grand Unification*, *Phys.Lett.* **B118** (1982) 73.
- [49] L. J. Hall, J. D. Lykken, and S. Weinberg, *Supergravity as the Messenger of Supersymmetry Breaking*, *Phys.Rev.* **D27** (1983) 2359–2378.
- [50] N. Ohta, *Grand Unified Theories Based on Local Supersymmetry*, *Prog.Theor.Phys.* **70** (1983) 542.
- [51] B. Allanach, *SOFTSUSY: a program for calculating supersymmetric spectra*, *Comput.Phys.Commun.* **143** (2002) 305–331, [[hep-ph/0104145](#)].
- [52] N. D. Christensen and C. Duhr, *FeynRules - Feynman rules made easy*, *Comput.Phys.Commun.* **180** (2009) 1614–1641, [[arXiv:0806.4194](#)].
- [53] C. Degrande, C. Duhr, B. Fuks, D. Grellscheid, O. Mattelaer, *et al.*, *UFO - The Universal FeynRules Output*, *Comput.Phys.Commun.* **183** (2012) 1201–1214, [[arXiv:1108.2040](#)].
- [54] J. Alwall, M. Herquet, F. Maltoni, O. Mattelaer, and T. Stelzer, *MadGraph 5 : Going Beyond*, *JHEP* **1106** (2011) 128, [[arXiv:1106.0522](#)].
- [55] W. Beenakker, R. Hopker, and M. Spira, *PROSPINO: A Program for the production of supersymmetric particles in next-to-leading order QCD*, [hep-ph/9611232](#).
- [56] T. Sjostrand, S. Mrenna, and P. Z. Skands, *PYTHIA 6.4 Physics and Manual*, *JHEP* **0605** (2006) 026, [[hep-ph/0603175](#)].

- [57] **ATLAS** Collaboration, G. Aad *et al.*, *Combined search for the Standard Model Higgs boson using up to 4.9 fb⁻¹ of pp collision data at with the ATLAS detector at the LHC*, *Physics Letters B* (Feb., 2012) [[arXiv:1202.1408](#)].
- [58] **CMS** Collaboration, S. Chatrchyan *et al.*, *Combined results of searches for the standard model Higgs boson in pp collisions at sqrt(s) = 7 TeV*, [arXiv:1202.1488](#).
- [59] J. Conway, “PGS - Pretty Good Simulation of high energy collisions.” <http://physics.ucdavis.edu/~conway/research/software/pgs/pgs4-general.htm>.
- [60] J. H. G. Landsberg, S. Jain, “Simple Limit Calculator.” http://www-d0.fnal.gov/Run2Physics/limit_calc/limit_calc.html.
- [61] **CMS** Collaboration, *Search for a missing energy signature from new physics in di-jet and multi-jet events*, . CMS-PAS-SUS-11-001.
- [62] **ATLAS** Collaboration, *Search for squarks and gluinos using final states with jets and missing transverse momentum with the ATLAS detector in sqrt(s) = 7 TeV proton-proton collisions*, [arXiv:1109.6572](#).
- [63] *Search for supersymmetry with jets and missing transverse momentum: Additional model interpretations*, Tech. Rep. ATLAS-CONF-2011-155, CERN, Geneva, Nov, 2011.
- [64] **ATLAS** Collaboration, G. Aad *et al.*, *Search for new phenomena in final states with large jet multiplicities and missing transverse momentum using sqrt(s) = 7 TeV pp collisions with the ATLAS detector*, *Journal of High Energy Physics* **2011** (Nov., 2011) [[arXiv:1110.2299](#)].
- [65] **CMS** Collaboration, S. Chatrchyan *et al.*, *Search for new physics with same-sign isolated dilepton events with jets and missing transverse energy*, [arXiv:1205.6615](#).
- [66] **CMS** Collaboration, S. Chatrchyan *et al.*, *Search for new physics with same-sign isolated dilepton events with jets and missing transverse energy at the LHC*, *JHEP* **1106** (2011) 077, [[arXiv:1104.3168](#)].
- [67] **CMS** Collaboration, *Search for new physics in events with a Z boson and missing energy*, .
- [68] **CMS** Collaboration, S. Chatrchyan *et al.*, *Search for anomalous production of multilepton events in pp collisions at sqrt(s)=7 TeV*, [arXiv:1204.5341](#).
- [69] **CMS** Collaboration, *Search for new physics in events with opposite-sign dileptons and missing transverse energy*, .
- [70] **ATLAS** Collaboration, G. Aad *et al.*, *Search for scalar bottom pair production with the ATLAS detector in pp Collisions at sqrt(s) = 7 TeV*, *Phys.Rev.Lett.* **108** (2012) 181802, [[arXiv:1112.3832](#)].
- [71] **ATLAS** Collaboration, G. Aad *et al.*, *Search for supersymmetry in pp collisions at sqrt(s) = 7 TeV in final states with missing transverse momentum and b-jets with the ATLAS detector*, *Phys.Rev.D* (2012) [[arXiv:1203.6193](#)].
- [72] **CMS** Collaboration, S. Chatrchyan *et al.*, *Search for new physics in events with same-sign dileptons and b-tagged jets in pp collisions at sqrt(s) = 7 TeV*, [arXiv:1205.3933](#).
- [73] **ATLAS** Collaboration, G. Aad *et al.*, *Searches for supersymmetry with the ATLAS detector using final states with two leptons and missing transverse momentum in sqrt(s) = 7 TeV proton-proton collisions*, *Phys.Lett.* **B709** (2012) 137–157, [[arXiv:1110.6189](#)].
- [74] **ATLAS** Collaboration, G. Aad *et al.*, *Search for supersymmetry in events with three leptons and missing transverse momentum in sqrt(s) = 7 TeV pp collisions with the ATLAS detector*, *Phys.Rev.Lett.* (2012) [[arXiv:1204.5638](#)].
- [75] M. Lisanti, P. Schuster, M. Strassler, and N. Toro, *Study of LHC Searches for a Lepton and Many Jets*, [arXiv:1107.5055](#).